RESEARCH ARTICLE

The exometabolome of microbial communities inhabiting bare ice surfaces on the southern Greenland Ice Sheet

Eva L. Doting[1,2] | Marie B. Jensen[1] | Elisa K. Peter[3,4] | Lea Ellegaard-Jensen[1] | Martyn Tranter[1] | Liane G. Benning[3,4] | Martin Hansen[1] | Alexandre M. Anesio[1]

[1]Department of Environmental Science, iClimate, Aarhus University, Roskilde, Denmark

[2]Department of Earth and Environmental Science, University of Pennsylvania, Philadelphia, Pennsylvania, USA

[3]Interface Geochemistry Section, German Research Centre for Geosciences, Potsdam, Germany

[4]Department of Earth Sciences, Freie Universität Berlin, Berlin, Germany

Correspondence
Eva L. Doting and Alexandre M. Anesio, Department of Earth and Environmental Science, University of Pennsylvania, Philadelphia, PA, USA.
Email: edoting@sas.upenn.edu; ama@envs.au.dk

Abstract

Microbial blooms colonize the Greenland Ice Sheet bare ice surface during the ablation season and significantly reduce its albedo. On the ice surface, microbes are exposed to high levels of irradiance, freeze–thaw cycles, and low nutrient concentrations. It is well known that microorganisms secrete metabolites to maintain homeostasis, communicate with other microorganisms, and defend themselves. Yet, the exometabolome of supraglacial microbial blooms, dominated by the pigmented glacier ice algae *Ancylonema alaskanum* and *Ancylonema nordenskiöldii*, remains thus far unstudied. Here, we use a high-resolution mass spectrometry-based untargeted metabolomics workflow to identify metabolites in the exometabolome of microbial blooms on the surface of the southern tip of the Greenland Ice Sheet. Samples were collected every 6 h across two diurnal cycles at 5 replicate sampling sites with high similarity in community composition, in terms of orders and phyla present. Time of sampling explained 46% (permutational multivariate analysis of variance [PERMANOVA], pseudo-$F = 3.7771$, $p = 0.001$) and 27% (PERMANOVA, pseudo-$F = 1.8705$, $p = 0.001$) of variance in the exometabolome across the two diurnal cycles. Annotated metabolites included riboflavin, lumichrome, tryptophan, and azelaic acid, all of which have demonstrated roles in microbe–microbe interactions in other ecosystems and should be tested for potential roles in the development of microbial blooms on bare ice surfaces.

INTRODUCTION

During the summer melt season, the bare ice ablation zone of the Greenland Ice Sheet becomes colonized by active microbial communities consisting of algae, protozoa, bacteria, fungi, and viruses (Anesio & Laybourn-Parry, 2012). These microbial blooms, dominated by the pigmented algae *Ancylonema alaskanum* and *Ancylonema nordenskiöldii* (Lutz et al., 2018; Procházková et al., 2021) have a significant effect on the darkening of the Greenland Ice Sheet (Ryan, 2017, 2018; Stibal et al., 2017; Uetake et al., 2010; Yallop et al., 2012). Controls on the development, spatial extent, and density of microbial blooms on bare ice surfaces remain poorly understood, causing large uncertainties in how microbial coverage of bare ice surfaces might change as snowlines retreat upwards due to climatic warming (Halbach et al., 2023; Ryan et al., 2019). Previous work has demonstrated that the availability of liquid water, light, and nutrients is essential for the development of these darkening algal blooms (Anesio et al., 2017; Holland et al., 2019; McCutcheon et al., 2021). In addition, it has been suggested that parasitic infections of glacier ice algae may

FIGURE 1 (A) Location of the 2021 field site on the southern Greenland Ice Sheet and (B) the dark ice surface where part of the samples in this study was collected.

limit the continued expansion of algal blooms as the melt season progresses (Perini et al., 2023). However, a metabolome-level understanding of microbial blooms on bare ice surfaces is currently lacking.

The supraglacial exometabolome is a reflection of the internal metabolic state of supraglacial microorganisms in response to their environmental conditions (Chubukov et al., 2014; Douglas, 2020; Krämer, 1994). More broadly speaking, the composition of the exometabolome is dependent on many factors, including the composition of the microbial community, the physiological state and growth phase of the community, and physicochemical parameters including temperature, the availability of (micro)nutrients, and light conditions (Barofsky et al., 2009; Engel et al., 2011; Grossart & Simon, 2007; Meon & Kirchman, 2001; Myklestad, 1995; Obernosterer & Herndl, 1995; Romera-Castillo et al., 2010; Wetz & Wheeler, 2007). Metabolites can be used in chemical signalling, which is used to coordinate the behaviour of unicellular microorganisms at the population level (Weisskopf et al., 2021). Metabolomics approaches have been used to study cryoconite holes in Greenland (Cook et al., 2016) and Svalbard (Gokul et al., 2023), and to assess differences between a red and a green snowfield on a glacier in Svalbard (Lutz et al., 2015). However, the supraglacial bare ice exometabolome and the dynamics thereof are still poorly characterized, preventing a fundamental understanding of bloom dynamics in such systems.

Here, we present the first analysis of the supraglacial exometabolome of microbial communities inhabiting bare ice surfaces on the southern Greenland Ice Sheet. Samples ($n = 48$) were collected at 10 different time points across two diurnal cycles to explore the diversity and dynamics of the supraglacial exometabolome. Metabolite data is linked to analysis of community composition and measurements of glacier ice algal photophysiology to explore microbial changes in response to diurnal variations in supraglacial conditions.

EXPERIMENTAL PROCEDURES

Site description

The Deep Purple (www.deeppurple-ercsyg.eu/home) 2021 base camp was established on the southern tip of the Greenland Ice Sheet at $\sim 61° 06'$ N, $46° 51'$ W between 12 July and 10 August 2021 (Figure 1A). A sampling area of 250×250 m was marked out upstream of the basecamp, where a range of measurements and sampling related to the biological darkening of the ice surface was conducted. All samples in this study were collected within a dedicated sector of the sampling area that was not disturbed by other sampling or camp activities. The sampling area was located ~ 1 km from the Programme for Monitoring of the Greenland Ice Sheet (PROMICE, www.promice.org) automatic weather station QAS_M, from which hourly meteorological data for air temperature, relative humidity, and shortwave radiation were obtained (Fausto et al., 2021; How et al., 2022).

Sample collection and field processing

On 16 and 26 July 2021, five replicate sites with visible biological darkening of the ice surface were marked within a ~ 10 m^2 subsection (Figure 1B) of the designated sampling sector. At noon on 16 and 26 July, on each day and at each replicate site, 50×50 cm of surface ice was collected into individual sterile WhirlPak bags, using an ethanol-wiped ice axe and trowel, which were preconditioned with clean surface ice prior to sample collection. Samples were taken to the field laboratory, where they were left to melt before filtering at least 200 mL of homogenized sample on a sterile Nalgene filtration unit (cellulose nitrate membrane, pore size 0.22 μm, Sartorius). Filters were transferred into cryotubes that were stored at $-80°$C on the ice and transported back to the home laboratory in a liquid nitrogen dry shipper and kept at $-80°$C until further processing for amplicon sequencing.

At the same time, a second 35 × 35 cm patch of surface ice at each replicate site was sampled in the same manner and taken back to the field lab for melting in a 10°C water bath. The samples were fully melted (within 20 min), and 22 mL of homogenized sample was filtered (glass microfiber, grade GF/F, Whatman) into a 50 mL Falcon tube. The filtrate was defined as containing the exometabolome and any biological activity was quenched by adding an equal volume (22 mL) of methanol (LC–MS Optima, Fisher Chemicals). Samples were stored at −20°C for transport back to Denmark until further processing. The WhirlPak bags containing the remaining sample were placed in the dark for dark adaptation prior to measurements by pulse amplitude modulated fluorometry (PAM; see section on PAM fluorometry).

Collection of samples for exometabolome analysis and PAM measurements was repeated every 6 h, until and including at noon the following day, yielding two sets (16-17 July and 26-27 July, referred to as diurnal cycles DC1 and DC2, respectively) of five timepoints each over 24 h, with five biological replicates each. Samples were collected as close together as possible to minimize the effect of spatial variation between samples collected at different time points while taking care to only sample untouched ice surfaces.

PAM fluorometry

The maximum photochemical efficiency of photosystem II in the dark-adapted state (F_v/F_m) was measured on a 3 mL sub-sample for each replicate, using a WaterPAM fluorometer (Walz GmBH). A blank adjustment was performed before measurements at each time point by filtering a 3 mL sample through a 0.2 μm syringe filter. Samples were dark-adapted for 30 min prior to F_v/F_m measurements. A stirrer in the cuvette with the sample was used to prevent the algal cells from sinking during each measurement.

Amplicon library preparation, sequencing, and bioinformatics

The cryo-preserved filters collected for microbial community composition analyses were thawed and extracted using the DNeasy PowerLyzer PowerSoil Kit (Qiagen). The cells were lysed by adding filters to the PowerBead tubes and using a Bead Ruptor Elite (Omni International, Inc, GA, USA). Hereafter, the extractions followed the manufacturer's protocol. For amplicon library preparation, a two-step polymerase chain reaction (PCR) approach was followed. The first PCR was used to amplify the region of interest, and the second to add indexes and sequencing adaptors. The V3 and V4 regions of the 16S rRNA gene were amplified for targeting the prokaryotic domain using 341F (5′-CCTAYGGGRBGCASCAG-3′) and 806R (5′- GGAC-TACNNGGGTATCTAAT-3′) primers. The V4 region of the 18S rRNA gene was amplified for targeting the eukaryotic community using 538F (5′- GCGGTAA TTCCAGCTCCAA-3′) and 706R (5′- AATCCRA-GAATTTCACCTCT-3′) primers. The first PCR was performed using 12.5 μL of 2XPCRBIO Ultra Mix (pcrbio, UK), 0.5 μL of 10 μM forward primer, 0.5 μL of 10 μM reverse primer, 6 μL nuclease-free water, 0.5 μL BSA, and 5 μL DNA template (1–10 ng/μL) to amplify the DNA fragments. The cycling conditions for amplifying both DNA fragments were: initial denaturation at 95°C for 2 min; 33 cycles at 95°C for 15 s, 55°C for 15 s, and 72°C for 40 s and a final extension at 72°C for 4 min. A second PCR was performed to add index primers using 12.5 μL 2XPCRBIO Ultra Mix (pcrbio, UK), 2 μL P5 index primer, 2 μL P7 index primer, 5.5 μL nuclease-free water, and 5 μL PCR product from the first PCR. Index primers were added using the cycling conditions: initial denaturation at 98°C for 1 min; 13 cycles at 98°C for 10 s, 55°C for 20 s, and 72°C for 40 s and a final extension at 72°C for 5 min. The resulting PCR products were purified with HighPrep™ PCR magnetic beads (MagBio Genomics Inc. Gaithersburg, Maryland, USA) and equimolarly pooled as two libraries: prokaryotic and eukaryotic. The libraries were sequenced at Aarhus University (Roskilde, Denmark) on a MiSeq Illumina instrument using the V2 kit (Illumina Inc. San Diego, California, USA) resulting in 2 × 250 bp reads.

All sequencing data were analysed using QIIME2 v2021.8 (Bolyen et al., 2019). Reads were denoised using the DADA2 denoised-paired plugin (Callahan et al., 2016). All the amplicon sequence variants (ASVs) were aligned using MAFFT (Katoh et al., 2002). Taxonomy was assigned to ASVs using the feature-classifier (Bokulich et al., 2018) against the SILVA 138 SSU Ref NR 99 database (Quast et al., 2013) to hereafter create community composition plots. For 16S and 18S rRNA data, all orders or phyla representing less than 1% relative abundance were pooled under 'Others'.

Nanoflow liquid chromatography high-resolution tandem mass spectrometry

Samples that were collected in 50 mL Falcon tubes were dried by placing the tubes in a SpeedVac (Christ, RVC 2-25 Cdplus with Christ CT 02-50 cold trap, 7 mbar, 40°C, 1000 rpm, 2 h) to remove all methanol, before freeze-drying (48 h, ScanVac CoolSafe, −110°C). Dried samples were reconstituted in 200 μL 5% methanol prior to analysis using an untargeted metabolomics workflow on a nano-liquid chromatography high-resolution tandem mass spectrometer (LC-

HRMS/MS), utilizing an UltiMate 3000 RSLCnano System (Dionex, ThermoFisher Scientific) hyphenated to a Q Exactive HF Orbitrap MS (ThermoFisher Scientific). The LC autosampler was kept at 8°C. For each sample, 1 μL sample was full-loop loaded onto an analytical column (PepMap RSLC C18, 75 μm × 150 mm, 3 μm, 40°C) at a 400 nL min^{-1} flow rate and a triple-phasic gradient (water and acetonitrile both with 0.1% formic acid) was applied over 40 min. Analytes were separated on the LC column, and then infused into the Orbitrap MS using an EASYspray nano-ion source, operated at a spray voltage of 1.80 kV in positive ionization mode, a capillary temperature of 250°C, a S-lens RF level of 50 V and a probe heater temperature of 350°C. The Orbitrap was operated in full scan at a mass resolution of 240,000 at 200 m/z, with the target automatic gain control set to 1e6 and a maximum injection time of 100 ms. Samples were scanned in the range of 90–1000 m/z. Quality control samples were prepared by pooling 45 μL of each sample (excluding procedural blanks) and were injected every fifth injection to monitor systematic errors and chromatographic performance, and to normalize for any changes in instrument performance during data acquisition.

In addition, the pooled quality control samples were also treated as samples for metabolite identification and were acquired with the data-dependent acquisition, and the 10 parent ions with the highest intensity were selected for MS/MS fragmentation (at 20 and 70 V normalized collision energy) in subsequent scans (i.e., Top10 mode). The MS2 scans were recorded at a mass resolution of 15,000 at 200 m/z, target automatic gain control set to 1e5, and a maximum injection time of 50 ms. The pooled QC sample was also injected to generate an iterative exclusion list that was applied during sample acquisition (Koelmel et al., 2018).

Metabolomics data processing

All spectral processing was performed in Compound Discoverer 3.3.2.31 (ThermoFisher Scientific). Spectra were aligned to that of a pooled QC sample injected in the middle of the data acquisition run and background-corrected using procedural blanks. Compound detection parameters were set to a mass tolerance of 2 ppm, a minimum peak intensity of 500,000, and a chromatographic signal-to-noise threshold of 1.5. Compounds were grouped using a mass tolerance of 2 ppm and a retention time tolerance of 0.5 min. Molecular formulae were assigned with a mass tolerance of 5 ppm, restricted to $C_{0-90}H_{0-190}N_{0-10}O_{0-18}P_{0-3}S_{0-5}$. Local databases (mzVault, ThermoFisher Scientific), mzCloud, and BioCyc (Karp et al., 2019) were searched for compound annotations. If a compound was detected, all chromatograms were searched again at an intensity threshold of 10,000, a mass tolerance of

2 ppm, and a signal-to-noise threshold of 1.5 to avoid the presence of missing values. Peak areas were normalized using pooled QC correction, where a linear regression model was applied to pooled QC samples injected throughout the data acquisition run. The QC correction was applied if a compound was detected in at least 25% of QC samples, had a maximum of 80% relative standard deviation within QC samples, and a maximum of 50% relative standard deviation within QC samples after correction. KEGG and BioCyc were searched for metabolic pathway matches with annotated compounds.

Assigned formulae were included if they were not marked as background, had normalized areas, and had a maximum annotated mass difference of ±2 ppm. Guidelines for annotation of metabolites, as outlined by the Metabolomics Standards Institute (Sumner et al., 2007; Viant et al., 2019), were applied. In short, peak integration and spectral matches to the in-house library were checked manually and Level 1 annotation (identified metabolite) was assigned for correctly assigned spectral matches and chromatographic retention time. Full matches to MzCloud were also manually inspected and were assigned Level 2 annotation (putatively annotated compound) for compounds with a match score >80. Remaining metabolites were assigned a Level 3 annotation (putatively characterized compound class) if fragmentation data were available but no match with a spectral library could be made, or a Level 4 annotation (unknown compound) for any compounds that did not meet the requirements outlined above.

Statistics

Normalized areas were exported from Compound Discoverer for further data analysis in R (R Core Team, 2020). Metabolite normalized areas were log-transformed and unit variance was scaled prior to principal component analysis (PCA) using the R package 'vegan' (Oksanen et al., 2011).

RESULTS

Rainfall, irradiance, and diurnal variation in glacier ice algal F_v/F_m

Weather conditions during the field campaign were highly variable, ranging from sunny to periods of heavy rain. Here, rainfall is reported based on personal observations, photos, and rainfall collection in a bucket on 18 and 19 July, as no PROMICE precipitation data are available for the study period. On 11 July (day of year (DOY) 192), rainfall (>8 h) partially stripped the weathering crust at the sampling site. This was followed by
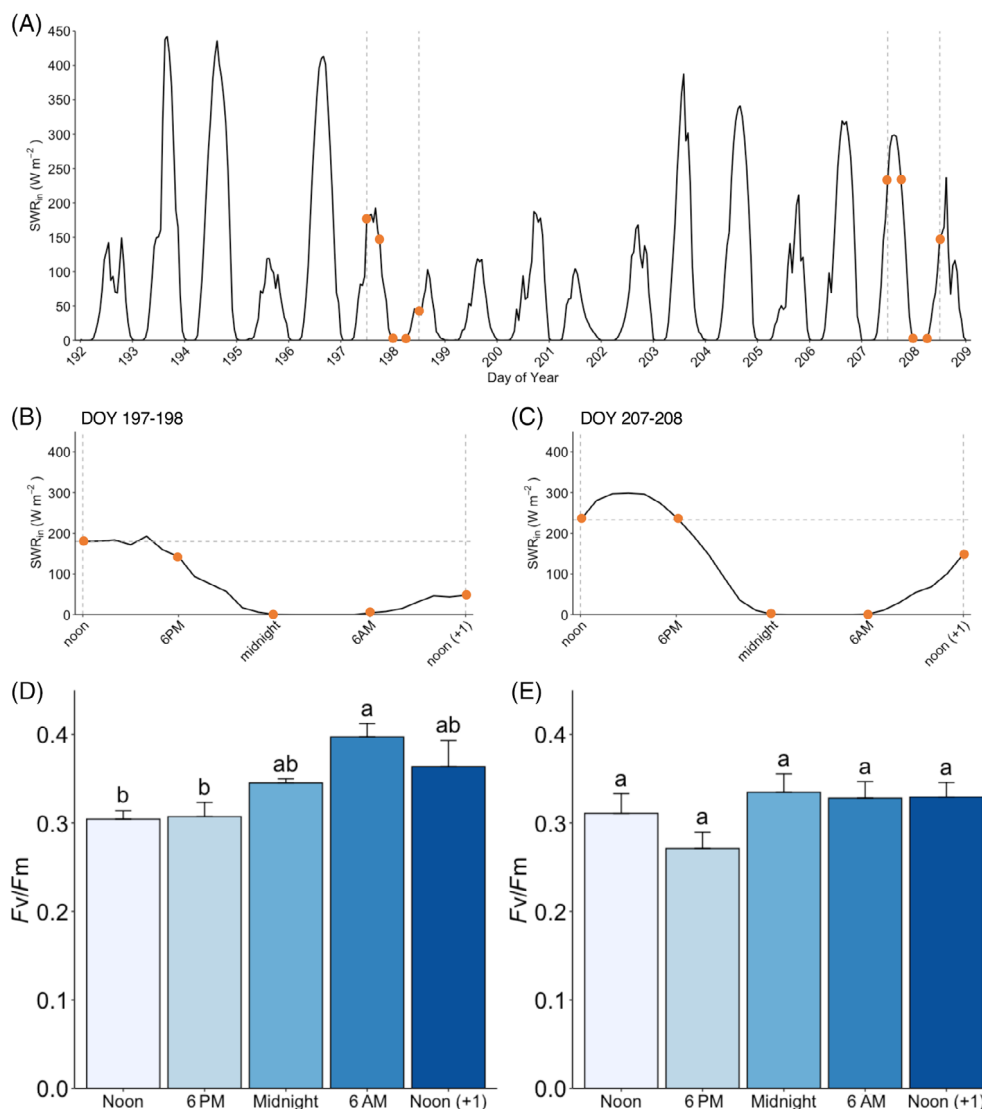
FIGURE 2 (A) Incoming shortwave radiation (SWR$_{in}$) in W m^{-2}, obtained from the PROMICE automatic weather station QAS_M, during the field campaign; (B) SWR$_{in}$ during DC1; and (C) SWR$_{in}$ during DC2. Dashed lines denote the timing of DC1 and DC2, and each sampled timepoint is denoted by an orange dot. (D) F_v/F_m measured for DC1 samples; (E) F_v/F_m measured for DC2 samples. Error bars denote the standard error ($n = 5$ per timepoint). Different letters on the bar plot indicate significant differences (Tukey post hoc, $p < 0.05$) in the pairwise comparisons within each diurnal cycle.

several overcast and/or sunny days with no significant rainfall, which allowed the weathering crust and associated microbial blooms to re-establish prior to sampling of DC1 on 16 July (DOY 197). Similarly, several large rain events (up to 50 mm day^{-1} locally) between 18 July (DOY 199) and the morning of 21 July (DOY 202) stripped the weathering crust again. At the start of sampling for DC2, the weathering crust had reformed as a result of 4 days with limited cloud cover (DOY 202–207).

During DC2, cumulative incoming shortwave radiation (SWR$_{in}$) was ~1.6-fold higher than cumulative SWR$_{in}$ during DC1 (Figure 2A–C). Cumulative SWR$_{in}$ in the 24 h prior to DC1 was ~2.3-fold higher than cumulative SWR$_{in}$ during DC1, while cumulative SWR$_{in}$

during the 24 h prior to DC2 was similar (1.2-fold higher) to cumulative SWR$_{in}$ during DC2. SWR$_{in}$ at noon was 3.8-fold and 1.6-fold higher than at noon (+1) in DC1 and DC2, respectively.

Maximum photochemical efficiency of photosystem II of glacier ice algae in the dark-adapted state (F_v/F_m) varied with time in DC1 (Kruskal–Wallis test, $p < 0.02$) but not in DC2 (Kruskal-Wallis test, $p > 0.2$) (Figure 2D,E). Across the measured time points, F_v/F_m ranged from 0.235 to 0.458, was highest at 6 AM in DC1 (0.40 ± 0.015), and lowest at 6 PM in DC2 (0.27 ± 0.018). Differences in F_v/F_m measured for biological replicates collected at the same timepoint ($n = 5$) were relatively high, with the standard error ranging from 0.005 to 0.03.
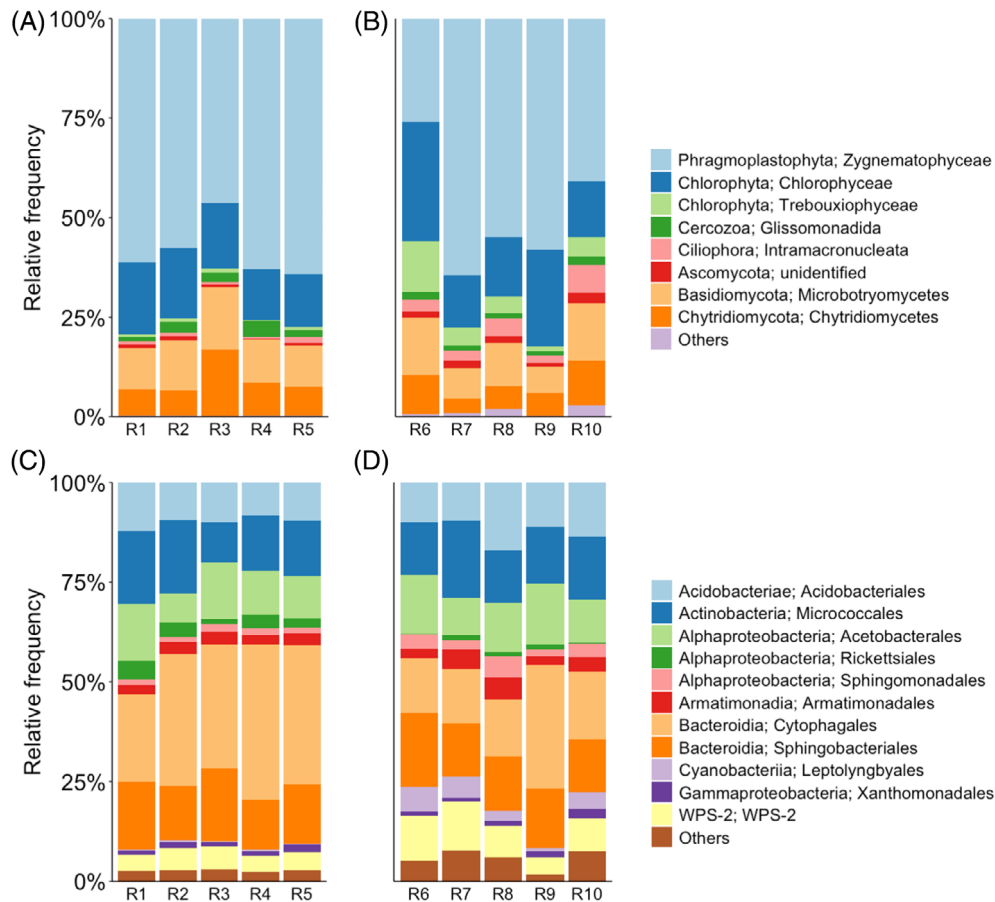
FIGURE 3 Relative abundance plots for (A) 18S amplicon sequencing data for replicate sites R1–R5 sampled at noon on the first sampling day of DC1, (B) 18S amplicon sequencing data for replicate sites R6–R10 sampled at noon on the first sampling day of DC2, (C) 16S amplicon sequencing data for replicate sites R1–R5 sampled at noon on the first sampling day of DC1 and (D) 16S amplicon sequencing data for replicate sites R6-R10 sampled at noon on the first sampling day of DC2.

Community composition

A significant fraction of the eukaryotic community (Figure 3A,B) sampled for both diurnal cycles was composed of algae, with representatives of *Zygnematophyceae* being the dominant organism in both DC1 (59% ± 7%) and DC2 (49% ± 15%). The remainder was made up of *Chlorophyta* (16% ± 3% in DC1 and 25% ± 10% in DC2), with a significantly larger ($p < 0.05$) contribution of *Trebouxiophyceae* in DC2 than in DC1. *Intramacronucleata* also had a significantly larger ($p < 0.05$) contribution to the eukaryotic community in DC2 than in DC1. Fungi, represented by *Ascomycota*, *Basidiomycota*, and *Chytridiomycota*, accounted for on average 22% ± 6% and 20% ± 7% of the eukaryotic community in DC1 and DC2, respectively. Only *Ascomycota* differed significantly ($p < 0.01$) between DC1 and DC2. Full eukaryotic community data can be found in Table S1.

The dominant class in the prokaryotic community (Figure 3C,D) was represented by *Bacteroidia*, which accounted for an average of 47% ± 5% and 33% ± 8% in DC1 and DC2, respectively. Contributions from both

Cytophagales ($p < 0.05$) and *Sphingomonadales* ($p < 0.05$) were significantly smaller in DC2 than in DC1. *Alphaproteobacteria* represented on average 16% ± 3% and 17% ± 3% of the prokaryotic community in DC1 and DC2, respectively, with *Rickettsiales* accounting for a significantly smaller ($p < 0.01$) percentage in DC2 than in DC1. Finally, cyanobacteria (*Leptolyngbyales*, $p < 0.01$) and *WPS-2* ($p < 0.05$) were significantly more abundant in DC2 than in DC1. Full prokaryotic community data can be found in Table S2.

Exometabolome of the glacier community

The use of a highly sensitive nanoflow LC-HRMS platform enabled us to detect 25,720 merged features that were assembled into 406 different substances with an assigned molecular formula (Table S3). After manual curation, 10 metabolites were annotated at Level 1 (identified metabolite), and 10 metabolites were annotated at Level 2 (putatively annotated compounds; Table 1). A further 331 substances were assigned a

TABLE 1 Annotated metabolites, their classification, and relevant biochemical pathway, if known, according to BioCyc (Karp et al., 2019) or KEGG (Kanehisa, 2019).

Names	Classification	Biochemical pathways
ID Level 1		
10-Hydroxydecanoic acid	Fatty acyl	
Adenine	Purine	Purine metabolism, nucleotide metabolism[a]
Azelaic acid	Fatty acyl	
Guanine	Purine	Purine metabolism, nucleotide metabolism[a]
Indole acrylic acid	Indole (auxin)	Tryptophan degradation[b]
Lumichrome	Flavin	Riboflavin metabolism[a]
Riboflavin	Flavin	Flavin biosynthesis in archaea, bacteria, and fungi[b]
Sebacic acid	Fatty acyl	
Tyrosine	Amino acid	Protein component, metabolite precursor[a, b]
Urocanic acid	Imidazole	Histidine metabolism[a]
ID Level 2		
7-methylguanine	Purine derivative	
Arginine	Amino acid	Protein component, metabolite precursor[a, b]
Cyclohexamine	Amine	
Glutamic acid	Amino acid	Protein component, metabolite precursor[a, b]
Hypoxanthine	Purine	Purine metabolism, nucleotide metabolism[a]
Leucine	Amino acid	Protein component, metabolite precursor[a, b]
Phenylalanine	Amino acid	Protein component, metabolite precursor[a, b]
Proline	Amino acid	Protein component, metabolite precursor[a, b]
Sulcatol	Fatty acyl	
Tryptophan	Amino acid	Protein component, metabolite precursor[a, b]

[a]Reported in KEGG.
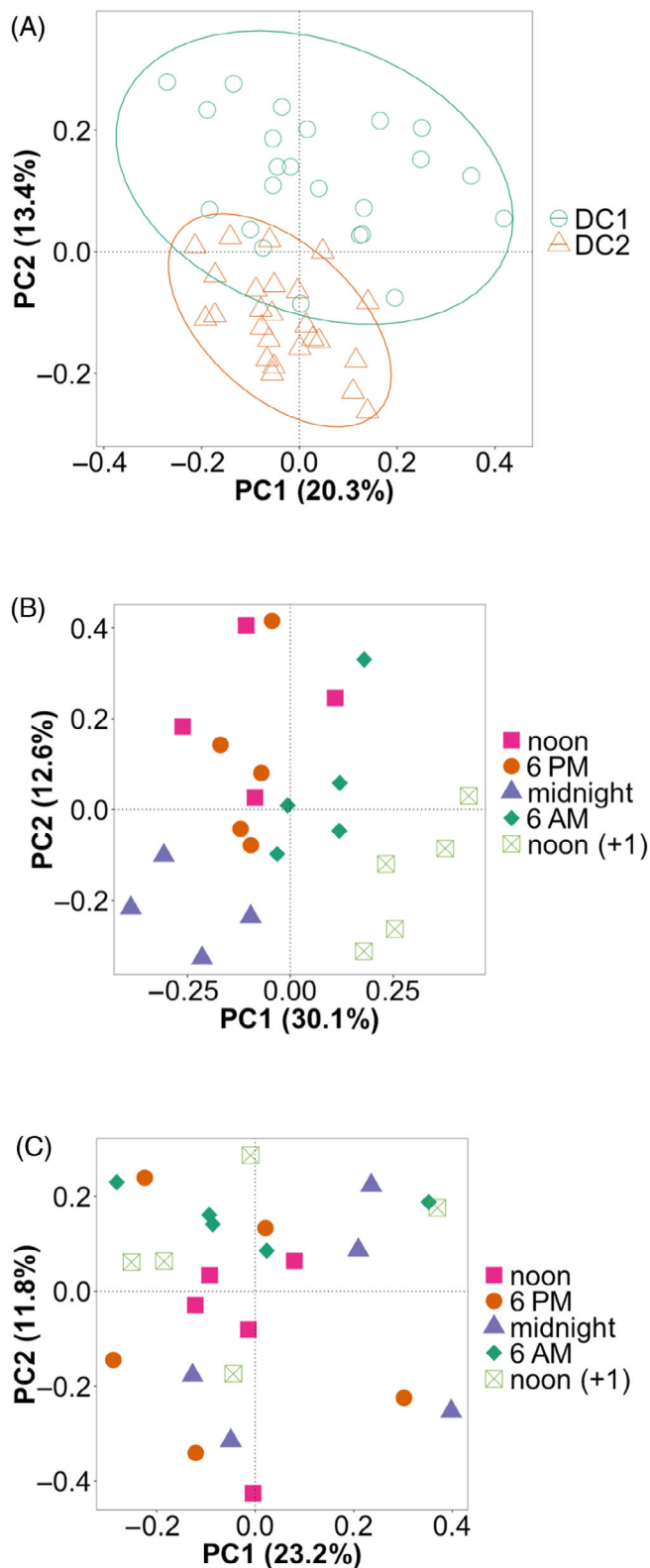[b]Reported in BioCyc.

FIGURE 4 (A) PCA scores plot of exometabolome profiles for DC1 and DC2, with ellipses showing 95% confidence intervals; (B) PCA scores plot of exometabolome profiles detected in DC1; and (C) PCA scores plot of exometabolome profiles detected in DC2. PCA is based on log-transformed and unit variance-scaled normalized areas of 406 metabolites.

Level 3 annotation (putatively characterized compound class) and the remaining substances (55) were assigned a Level 4 annotation (unknown compounds).

PCA of the detected metabolites showed that there is a small difference between the exometabolome profiles detected in DC1 and DC2 (33.7% of variance explained by the first two principal components, Figure 4A). Permutational multivariate analysis of variance (PERMANOVA) showed that the date of sampling (DC1 vs. DC2) significantly affected the exometabolome but only explained 15% of the variance (pseudo-$F = 8.3033$, $p = 0.001$, $R^2 = 0.15$). In DC1, the first two principal components explained 42.7% of the variance between exometabolome profiles detected at different time points (Figure 4B). The exometabolite profile of samples collected at midnight differed from the exometabolome at noon ($+1$) along PC1, and both clustered separately from the other three time points along PC2. The time of sampling significantly affected the exometabolome in DC1 and explained 46% of the observed variance (PERMANOVA, pseudo-$F = 3.7771$, $p = 0.001$, $R^2 = 0.46$). In DC2, 35% of the variance was captured by PC1 and PC2, but exometabolomes did not cluster by the time of sampling. Similar to DC1, the time of sampling significantly affected the exometabolite profile in DC2, but the effect size and variance explained were lower than in DC1 (PERMANOVA, pseudo-$F = 1.8705$, $p = 0.001$, $R^2 = 0.27$). Irradiance at the time of sampling alone, ignoring light history, explained 9% of variance in both DC1 (PERMANOVA, pseudo-$F = 2.1795$, $p = 0.037$, $R^2 = 0.09$) and DC2 (PERMANOVA, pseudo-$F = 2.2057$, $p = 0.021$, $R^2 = 0.09$).

DISCUSSION

In this study, we examined the diversity and dynamics of the exometabolome of microbial communities inhabiting the bare ice ablation zone of the southern Greenland Ice Sheet over two diurnal cycles. Because of the limited availability of nutrients on bare ice surfaces, tight recycling of dissolved organic matter within supraglacial microbial blooms has been assumed. This first characterization of the bare ice surface exometabolome, which contains metabolites that have important roles in microbe–microbe interactions in other ecosystems, implies that chemical signalling likely plays an unexplored role in the progression and spatial distribution of supraglacial microbial blooms.

Irradiance and glacier ice algae photophysiology

Environmental stressors for algae living in icy habitats include irradiance, freeze–thaw cycles, and changes in nutrient availability or salinity as a result of partial refreezing of surface water (Amato et al., 2009; De Vries et al., 2018; Joly et al., 2015; Mader et al., 2006; Wilson et al., 2012; Zhang et al., 2020). All of these factors can affect the photochemical efficiency of photosystem II (F_v/F_m) of glacier ice algae in the dark-adapted state. Ambient levels of irradiance on the Greenland Ice Sheet were shown to suppress glacier algae photochemistry relative to incubations at lower levels of irradiance (Williamson et al., 2020). In DC1, we observe a similar response, with a lower F_v/F_m at noon and 6 PM than at 6 AM (Figure 2C), where irradiance and cumulative photo-dose effect are lowest. Yet, in DC2, no significant changes in F_v/F_m with time were observed. This may be due to high variability in F_v/F_m measurements of biological replicates, potentially as a result of the heterogeneity of bare ice surfaces, the potential for local differences in nutrient or water availability, or natural variability associated with cell orientation, size, pigment content or pigment packaging effects (Chevrollier et al., 2023). Samples collected in DC2 were subject to similar levels of irradiance in the 24 h prior to sampling and on the sampling day itself, so acclimation to light conditions may have reduced variation in F_v/F_m during DC2. Data to assess the potential effect of environmental stressors other than irradiance are not available, so this study does not allow us to discern the major driving force of changes, or lack thereof, in F_v/F_m over time.

Community composition

The microbial community at replicate sites within each diurnal cycle was comparable in terms of community composition, and similar to that found for Greenland Ice Sheet dark ice surfaces in previous studies, in terms of detected phyla and classes (Lutz et al., 2018; Musilova et al., 2015; Perini et al., 2019; Stibal et al., 2017; Williamson et al., 2018; Yallop et al., 2012). However, when comparing the two diurnal cycles, the relative abundance of *Trebouxiophyceae*, *Intramacronucleata*, *Ascomycota*, *Leptolyngbyales*, and *WPS-2* was significantly higher in DC2 than in DC1. Differences in relative abundance are expected to produce different exometabolite profiles, as different organisms produce different metabolites, and chemical signalling between microbes can be density dependent.

Sampling the supraglacial exometabolome

Next to factors such as irradiance, community composition, nutrient availability, and heterogeneity of ice surfaces, the collection and processing of samples for supraglacial metabolomics is likely to introduce variation in the data obtained. The porosity of the weathering crust is highly variable, making it impossible to control

sampling depth when scraping off the top centimetre(s) of the ice surface that hosts the microbial communities of interest. This leads to variable dilution of collected samples and renders the comparison of concentrations of individual metabolites between samples impossible, even when normalizing to cell counts or DNA concentrations. Yet, just like for the relative abundance of bacteria and algae, exometabolite profiles based on peak area for different metabolites can be compared to assess relative differences between samples.

The fact that bare ice surface microbial communities are associated with ice crystals further complicates the analysis of the exometabolome, as collected samples need to be melted before they can be processed (i.e., filtration and quenching of microbial activity). This can either be done at ambient temperatures, which would keep the samples inside a bag, and in nonambient light conditions, both of which are likely to alter the (exo)metabolome. Alternatively, as was done in this study, a water bath can be used to expedite the melting process and reduce the time between sampling and sample processing. The 10°C water bath raised the water temperatures inside sampling bags to a maximum of 4.6 ± 0.6°C over the 20 min it took to melt the samples. This is a higher temperature than is experienced by bare ice surface microbes in their natural environment, which is also likely to affect the internal metabolic state and exometabolome of the sampled microbes. Despite our inability to control for these and other factors that are likely to induce variability in the supraglacial exometabolome, it is valuable to identify metabolites that are present in environmental samples so that they may subsequently be tested in more controlled lab experiments using recently established cultures of glacier ice algae (Jensen et al., 2023; Remias & Procházková, 2023).

Bare ice surface exometabolites

Several of the 20 annotated metabolites found in the exometabolome of microbial communities inhabiting bare ice surfaces have known roles in microbe–microbe interactions in other ecosystems. Here, we briefly highlight some of the metabolites that could be of particular interest for future research on the role of chemical signalling in the dynamics and development of microbial blooms on bare ice surfaces, either in situ or in recently established lab cultures (Jensen et al., 2023; Remias & Procházková, 2023).

Indole acrylic acid is an indole derivative that has been detected in a red macroalga and a Gram-negative bacterium (Davyt et al., 1998; Wlodarska et al., 2017). It is an auxin that, similar to the most abundant member of the auxin family of phytohormones, indole 3-acetic acid, has tryptophan as its main precursor (Wlodarska

et al., 2017). Indole 3-acetic acid has been detected in the exometabolome of various freshwater and marine bacteria and was found to be a growth factor of green algae and a diatom (Amin et al., 2015; Bagwell et al., 2014; Fiore et al., 2015; Labeeuw et al., 2016; Segev et al., 2016; Wienhausen et al., 2017; Zhang et al., 2014). Given the presence of green algae, *Alphaproteobacteria*, and cyanobacteria in bare ice surface microbial communities, the potential role of tryptophan and indole acrylic acid as a growth factor in supraglacial communities should be explored further.

Bacteria can produce lumichrome and riboflavin, which were found to promote algal growth in several studies (Brisson et al., 2021; Heo et al., 2019; Lopez et al., 2019; Peng et al., 2021). *Chlamydomonas reinhardtii* (*Chlorophyta*) also produces lumichrome, which was found to stimulate the *Pseudomonas aeruginosa* (*Gammaproteobacteria*) LasR quorum sensing receptor (Rajamani et al., 2008). In addition, bacterially produced riboflavin and lumichrome were found to mitigate salt stress in the freshwater microalga *Chlorella sorokiniana* (*Chlorophyta*; Palacios et al., 2021). Representatives of *Chlorophyta* and *Gammaproteobacteria* are part of the bare ice surface microbial community, and so further research into the ability of these glacier surface microorganisms to produce or sense riboflavin and lumichrome is of interest to better understand microbial interactions, as well as algal stress mitigation mechanisms.

Bacterial response to azelaic acid is controlled by the transcriptional regulator AzeR (Bez et al., 2020). A search of publicly available bacterial genomes found that the presence of AzeR is mostly limited to the *Proteobacteria* phylum (Shibl et al., 2020), which accounted for on average 16% ± 3% of the bacterial community in the present study. Hence, azelaic acid may be a metabolite of interest for future studies into chemical signalling in surface ice microbial communities.

AUTHOR CONTRIBUTIONS
Eva L. Doting: Conceptualization (lead); data curation (lead); formal analysis (lead); investigation (lead); methodology (lead); writing—original draft (lead); writing—review and editing (lead). **Marie B. Jensen:** Formal analysis (equal); methodology (equal); writing—original draft (supporting); writing—review and editing (equal). **Elisa K. Peter:** Conceptualization (equal); methodology (equal); writing—review and editing (equal). **Lea Ellegaard-Jensen:** Methodology (supporting); resources (supporting); writing—review and editing (equal). **Martyn Tranter:** Funding acquisition (lead); writing—review and editing (equal). **Liane G. Benning:** Conceptualization (supporting); funding acquisition (lead); writing—review and editing (equal). **Martin

CONFLICT OF INTEREST STATEMENT
The authors declare no conflicts of interest.

DATA AVAILABILITY STATEMENT
Sequencing data are openly available at the NCBI Sequence Read Archive under BioProject ID PRJNA980660 and BioSample accession numbers SAMN35639454 and SAMN35639455; https://www.ncbi.nlm.nih.gov/bioproject/PRJNA980660.

ORCID
Eva L. Doting https://orcid.org/0000-0002-2195-8299

REFERENCES
Amato, P., Doyle, S. & Christner, B.C. (2009) Macromolecular synthesis by yeasts under frozen conditions. *Environmental Microbiology*, 11(3), 589–596. Available from: https://doi.org/10.1111/j.1462-2920.2008.01829.x

Amin, S.A., Hmelo, L.R., Van Tol, H.M., Durham, B.P., Carlson, L.T., Heal, K.R. et al. (2015) Interaction and signaling between a cosmopolitan phytoplankton and associated bacteria. *Nature*, 522(7554), 98–101. Available from: https://doi.org/10.1038/nature14488

Anesio, A.M. & Laybourn-Parry, J. (2012) Glaciers and ice sheets as a biome. *Trends in Ecology and Evolution*, 27, 219–225. Available from: https://doi.org/10.1016/j.tree.2011.09.012

Anesio, A.M., Lutz, S., Chrismas, N.A.M. & Benning, L.G. (2017) The microbiome of glaciers and ice sheets. *npj Biofilms Microbiomes*, 3, 10. https://doi.org/10.1038/s41522-017-0019-0

Bagwell, C.E., Piskorska, M., Soule, T., Petelos, A. & Yeager, C.M. (2014) A diverse assemblage of indole-3-acetic acid producing bacteria associate with unicellular green algae. *Applied Biochemistry and Biotechnology*, 173(8), 1977–1984. Available from: https://doi.org/10.1007/S12010-014-0980-5/FIGURES/3

Barofsky, A., Vidoudez, C. & Pohnert, G. (2009) Metabolic profiling reveals growth stage variability in diatom exudates. *Limnology and Oceanography: Methods*, 7(6), 382–390. Available from: https://doi.org/10.4319/LOM.2009.7.382

Bez, C., Javvadi, S.G., Bertani, I., Devescovi, G., Guarnaccia, C., Studholme, D.J. et al. (2020) AzeR, a transcriptional regulator that responds to azelaic acid in pseudomonas nitroreducens. *Microbiology*, 166(1), 73–84. Available from: https://doi.org/10.1099/MIC.0.000865

Bokulich, N.A., Kaehler, B.D., Rideout, J.R., Dillon, M., Bolyen, E., Knight, R. et al. (2018) Optimizing taxonomic classification of marker-gene amplicon sequences with QIIME 2's q2-feature-classifier plugin. *Microbiome*, 6(1), 1–17. Available from: https://doi.org/10.1186/S40168-018-0470-Z/TABLES/3

Bolyen, E., Rideout, J.R., Dillon, M.R., Bokulich, N.A., Abnet, C.C., Al-Ghalith, G.A. et al. (2019) Reproducible, interactive, scalable and extensible microbiome data science using QIIME 2. *Nature Biotechnology*, 37(8), 852–857. Available from: https://doi.org/10.1038/s41587-019-0209-9

Brisson, V., Mayali, X., Bowen, B., Golini, A., Thelen, M., Stuart, R.K. et al. (2021) Identification of effector metabolites using exometabolite profiling of diverse microalgae. *mSystems*, 6(6), e0083521. Available from: https://doi.org/10.1128/MSYSTEMS.00835-21/SUPPL_FILE/MSYSTEMS.00835-21-ST002.XLSX

Callahan, B.J., McMurdie, P.J., Rosen, M.J., Han, A.W., Johnson, A.J.A. & Holmes, S.P. (2016) DADA2: high-resolution sample inference from Illumina amplicon data. *Nature Methods*, 13(7), 581–583. Available from: https://doi.org/10.1038/NMETH.3869

Chevrollier, L.A., Cook, J.M., Halbach, L., Jakobsen, H., Benning, L.G., Anesio, A.M. et al. (2023) Light absorption and albedo reduction by pigmented microalgae on snow and ice. *Journal of Glaciology*, 69(274), 333–341. Available from: https://doi.org/10.1017/jog.2022.64

Chubukov, V., Gerosa, L., Kochanowski, K. & Sauer, U. (2014) Coordination of microbial metabolism. *Nature Reviews Microbiology*, 12(5), 327–340. Available from: https://doi.org/10.1038/nrmicro3238

Cook, J.M., Edwards, A., Bulling, M., Mur, L.A.J., Cook, S., Gokul, J.K. et al. (2016) Metabolome-mediated biocryomorphic evolution promotes carbon fixation in Greenlandic cryoconite holes. *Environmental Microbiology*, 18(12), 4674–4686. Available from: https://doi.org/10.1111/1462-2920.13349

Davyt, D., Entz, W., Fernandez, R., Mariezcurrena, R., Mombru, A.W., Saldana, J. et al. (1998) A new indole derivative from the red alga Chondria atropurpurea. Isolation, structure determination, and anthelmintic activity. *Journal of Natural Products*, 61(12), 1560–1563. Available from: https://doi.org/10.1021/NP980114C/ASSET/IMAGES/LARGE/NP980114CF00001.JPEG

De Vries, J., Curtis, B.A., Gould, S.B. & Archibald, J.M. (2018) Embryophyte stress signaling evolved in the algal progenitors of land plants. *Proceedings of the National Academy of Sciences of the United States of America*, 115(15), E3471–E3480. Available from: https://doi.org/10.1073/pnas.1719230115

Douglas, A.E. (2020) The microbial exometabolome: ecological resource and architect of microbial communities. *Philosophical Transactions of the Royal Society of London Series B Biological Sciences*, 375(1798), 20190250. Available from: https://doi.org/10.1098/rstb.2019.0250

Engel, A., Händel, N., Wohlers, J., Lunau, M., Grossart, H.P., Sommer, U. et al. (2011) Effects of sea surface warming on the production and composition of dissolved organic matter during phytoplankton blooms: results from a mesocosm study. *Journal of Plankton Research*, 33(3), 357–372. Available from: https://doi.org/10.1093/PLANKT/FBQ122

Fausto, R.S., Van As, D., Mankoff, K.D., Vandecrux, B., Citterio, M., Ahlstrøm, A.P. et al. (2021) Programme for Monitoring of the Greenland Ice Sheet (PROMICE) automatic weather station data. *Earth System Science Data*, 13(8), 3819–3845. Available from: https://doi.org/10.5194/ESSD-13-3819-2021

Fiore, C.L., Longnecker, K., Kido Soule, M.C. & Kujawinski, E.B. (2015) Release of ecologically relevant metabolites by the cyanobacterium Synechococcus elongatus CCMP 1631. *Environmental Microbiology*, 17(10), 3949–3963. Available from: https://doi.org/10.1111/1462-2920.12899/SUPPINFO

Gokul, J.K., Mur, L.A.J., Hodson, A.J., Aliyah, T.D.L.I. & Nozomu, R.D. (2023) Icescape-scale metabolomics reveals cyanobacterial and topographic control of the core metabolism of the cryoconite ecosystem of an Arctic ice cap. *Environmental Microbiology*, 25(11), 2549–2563. Available from: https://doi.org/10.1111/1462-2920.16485

Grossart, H.P. & Simon, M. (2007) Interactions of planktonic algae and bacteria: effects on algal growth and organic matter dynamics. *Aquatic Microbial Ecology*, 47(2), 163–176. Available from: https://doi.org/10.3354/AME047163

Halbach, L., Chevrollier, L.-A., Cook, J.M., Stevens, I.T., Hansen, M., Anesio, A.M. et al. (2023) Dark ice in a warming world: advances and challenges in the study of Greenland Ice Sheet's biological darkening. *Annals of Glaciology*, 63, 1–6. Available from: https://doi.org/10.1017/aog.2023.17

Heo, J., Kim, S., Cho, D.H., Song, G.C., Kim, H.S. & Ryu, C.M. (2019) Genome-wide exploration of Escherichia coli genes to promote *Chlorella vulgaris* growth. *Algal Research*, 38, 101390. Available from: https://doi.org/10.1016/J.ALGAL.2018.101390

Holland, A.T., Williamson, C.J., Sgouridis, F., Tedstone, A.J., McCutcheon, J., Cook, J.M. et al. (2019) Dissolved organic nutrients dominate melting surface ice of the dark zone (Greenland Ice Sheet). *Biogeosciences*, 16(16), 3283–3296. Available from: https://doi.org/10.5194/bg-16-3283-2019

How, P., Abermann, J., Ahlstrøm, A. P., Andersen, S. B., Box, J. E., Citterio, M. et al. (2022). PROMICE and GC-Net automated weather station data in Greenland [Data set]. GEUS Dataverse. https://doi.org/10.22008/FK2/IW73UU

Jensen, M.B., Perini, L., Halbach, L., Jakobsen, H., Haraguchi, L., Ribeiro, S. et al. (2023) The dark art of cultivating glacier ice algae. *Botany Letters*. Available from: https://doi.org/10.1080/23818107.2023.2248235

Joly, M., Amato, P., Sancelme, M., Vinatier, V., Abrantes, M., Deguillaume, L. et al. (2015) Survival of microbial isolates from clouds toward simulated atmospheric stress factors. *Atmospheric Environment*, 117, 92–98. Available from: https://doi.org/10.1016/J.ATMOSENV.2015.07.009

Kanehisa, M. (2019) Toward understanding the origin and evolution of cellular organisms. *Protein Science*, 28(11), 1947–1951. Available from: https://doi.org/10.1002/PRO.3715

Karp, P.D., Billington, R., Caspi, R., Fulcher, C.A., Latendresse, M., Kothari, A. et al. (2019) The BioCyc collection of microbial genomes and metabolic pathways. *Briefings in Bioinformatics*, 20(4), 1085–1093. Available from: https://doi.org/10.1093/BIB/BBX085

Katoh, K., Misawa, K., Kuma, K.I. & Miyata, T. (2002) MAFFT: a novel method for rapid multiple sequence alignment based on fast Fourier transform. *Nucleic Acids Research*, 30(14), 3059–3066. Available from: https://doi.org/10.1093/NAR/GKF436

Koelmel, J.P., Kroeger, N.M., Gill, E.L., Ulmer, C.Z., John, A., Patterson, R.E. et al. (2018) Acquisition with automated exclusion list generation. *Journal of the American Society for Mass Spectrometry*, 28(5), 908–917. Available from: https://doi.org/10.1007/s13361-017-1608-0.Expanding

Krämer, R. (1994) Secretion of amino acids by bacteria: physiology and mechanism. *FEMS Microbiology Reviews*, 13(1), 75–93. Available from: https://doi.org/10.1111/J.1574-6976.1994.TB00036.X

Labeeuw, L., Khey, J., Bramucci, A.R., Atwal, H., De La Mata, A.P., Harynuk, J. et al. (2016) Indole-3-acetic acid is produced by Emiliania huxleyi coccolith-bearing cells and triggers a physiological response in bald cells. *Frontiers in Microbiology*, 7(6), 828. Available from: https://doi.org/10.3389/FMICB.2016.00828/BIBTEX

Lopez, B.R., Palacios, O.A., Bashan, Y., Hernández-Sandoval, F.E. & De-Bashan, L.E. (2019) Riboflavin and lumichrome exuded by the bacterium Azospirillum brasilense promote growth and changes in metabolites in Chlorella sorokiniana under autotrophic conditions. *Algal Research*, 44, 101696. Available from: https://doi.org/10.1016/J.ALGAL.2019.101696

Lutz, S., Anesio, A.M., Field, K. & Benning, L.G. (2015) Integrated "omics", targeted metabolite and single-cell analyses of arctic snow algae functionality and adaptability. *Frontiers in Microbiology*, 6(11), 1–17. Available from: https://doi.org/10.3389/fmicb.2015.01323

Lutz, S., McCutcheon, J., McQuaid, J.B. & Benning, L.G. (2018) The diversity of ice algal communities on the Greenland Ice Sheet as revealed by oligotyping. *Microbial Genomics*, 4(3), e000159. Available from: https://doi.org/10.1099/MGEN.0.000159/CITE/REFWORKS

Mader, H.M., Pettitt, M.E., Wadham, J.L., Wolff, E.W. & Parkes, R.J. (2006) Subsurface ice as a microbial habitat. *Geology*, 34(3), 169–172. Available from: https://doi.org/10.1130/G22096.1

McCutcheon, J., Lutz, S., Williamson, C., Cook, J.M., Tedstone, A.J., Vanderstraeten, A. et al. (2021) Mineral phosphorus drives glacier algal blooms on the Greenland Ice Sheet. *Nature Communications*, 12(1), 1–11. Available from: https://doi.org/10.1038/s41467-020-20627-w

Meon, B. & Kirchman, D.L. (2001) Dynamics and molecular composition of dissolved organic material during experimental phytoplankton blooms. *Marine Chemistry*, 75(3), 185–199. Available from: https://doi.org/10.1016/S0304-4203(01)00036-6

Musilova, M., Tranter, M., Bennett, S.A., Wadham, J. & Anesio, A.M. (2015) Stable microbial community composition on the Greenland Ice Sheet. *Frontiers in Microbiology*, 6(3), 193. Available from: https://doi.org/10.3389/fmicb.2015.00193

Myklestad, S.M. (1995) Release of extracellular products by phytoplankton with special emphasis on polysaccharides. *Science of the Total Environment*, 165(1–3), 155–164. Available from: https://doi.org/10.1016/0048-9697(95)04549-G

Obernosterer, I. & Herndl, G.J. (1995) Phytoplankton extracellular release and bacterial growth: Dependence on the inorganic N:P ratio. *Marine Ecology Progress Series*, 116(1–3), 247–258. Available from: https://doi.org/10.3354/meps116247

Oksanen, A.J., Blanchet, F.G., Friendly, M., Kindt, R., Legendre, P., Mcglinn, D. et al. (2011) Vegan: community ecology package.

Palacios, O.A., López, B.R., Palacios-Espinosa, A., Hernández-Sandoval, F.E. & De-Bashan, L.E. (2021) The immediate effect of riboflavin and lumichrome on the mitigation of saline stress in the microalga Chlorella sorokiniana by the plant-growth-promoting bacterium Azospirillum brasilense. *Algal*

Research, 58, 102424. Available from: https://doi.org/10.1016/J.ALGAL.2021.102424

Peng, H., De-Bashan, L.E. & Higgins, B.T. (2021) Comparison of algae growth and symbiotic mechanisms in the presence of plant growth promoting bacteria and non-plant growth promoting bacteria. *Algal Research*, 53, 102156. Available from: https://doi.org/10.1016/J.ALGAL.2020.102156

Perini, L., Gostinčar, C., Anesio, A.M., Williamson, C., Tranter, M. & Gunde-Cimerman, N. (2019) Darkening of the Greenland Ice Sheet: fungal abundance and diversity are associated with algal bloom. *Frontiers in Microbiology*, 10(3), 1–14. Available from: https://doi.org/10.3389/fmicb.2019.00557

Perini, L., Gostinčar, C., Likar, M., Frisvad, J.C., Kostanjšek, R., Nicholes, M. et al. (2023) Interactions of fungi and algae from the Greenland Ice Sheet. *Microbial Ecology*, 86(1), 282–296. Available from: https://doi.org/10.1007/s00248-022-02033-5

Procházková, L., Řezanka, T., Nedbalová, L. & Remias, D. (2021) Unicellular versus filamentous: the glacial alga Ancylonema alaskana comb. et stat. Nov. and its Ecophysiological relatedness to *Ancylonema nordenskioeldii* (Zygnematophyceae, Streptophyta). *Microorganisms*, 9(5), 1103. Available from: https://doi.org/10.3390/MICROORGANISMS9051103

Quast, C., Pruesse, E., Yilmaz, P., Gerken, J., Schweer, T., Yarza, P. et al. (2013) The SILVA ribosomal RNA gene database project: improved data processing and web-based tools. *Nucleic Acids Research*, 41(D1), D590–D596. Available from: https://doi.org/10.1093/NAR/GKS1219

R Core Team. (2020) *R: a language and environment for statistical computing*. Vienna, Austria: R Foundation for Statistical Computing. https://www.r-project.org/

Rajamani, S., Bauer, W.D., Robinson, J.B., Farrow, J.M., Pesci, E.C., Teplitski, M. et al. (2008) The vitamin riboflavin and its derivative lumichrome activate the LasR bacterial quorum-sensing receptor. *Molecular Plant-Microbe Interactions*, 21(9), 1184–1192. Available from: https://doi.org/10.1094/MPMI-21-9-1184

Remias, D. & Procházková, L. (2023) The first cultivation of the glacier ice alga Ancylonema alaskanum (Zygnematophyceae, Streptophyta): differences in morphology and photophysiology of field vs laboratory strain cells. *Journal of Glaciology*, 69(276), 1080–1084. Available from: https://doi.org/10.1017/jog.2023.22

Romera-Castillo, C., Sarmento, H., Álvarez-Salgado, X.A., Gasol, J.M. & Marrasé, C. (2010) Production of chromophoric dissolved organic matter by marine phytoplankton. *Limnology and Oceanography*, 55(1), 446–454. Available from: https://doi.org/10.4319/LO.2010.55.1.0446

Ryan, J. (2017) Derivation of high spatial resolution albedo from UAV digital imagery: application over the Greenland Ice Sheet. *Frontiers in Earth Science*, 5, 00040. Available from: https://doi.org/10.3389/feart.2017.00040

Ryan, J.C. (2018) Dark zone of the Greenland Ice Sheet controlled by distributed biologically-active impurities. *Nature Communications*, 9(1), 1065. Available from: https://doi.org/10.1038/s41467-018-03353-2

Ryan, J.C., Smith, L.C., Van As, D., Cooley, S.W., Cooper, M.G., Pitcher, L.H. et al. (2019) Greenland Ice Sheet surface melt amplified by snowline migration and bare ice exposure. *Science Advances*, 5(3), eaav3738. Available from: https://doi.org/10.1126/SCIADV.AAV3738/SUPPL_FILE/AAV3738_SM.PDF

Segev, E., Wyche, T.P., Kim, K.H., Petersen, J., Ellebrandt, C., Vlamakis, H. et al. (2016) Dynamic metabolic exchange governs a marine algal-bacterial interaction. *eLife*, 5(11), e17473. Available from: https://doi.org/10.7554/ELIFE.17473

Shibl, A.A., Isaac, A., Ochsenkühn, M.A., Cárdenas, A., Fei, C., Behringer, G. et al. (2020) Diatom modulation of select bacteria through use of two unique secondary metabolites. *Proceedings of the National Academy of Sciences of the United States of America*, 117(44), 27445–27455. Available from: https://doi.org/10.1073/PNAS.2012088117

Stibal, M., Box, J.E., Cameron, K.A., Langen, P.L., Yallop, M.L., Mottram, R.H. et al. (2017) Algae drive enhanced darkening of bare ice on the Greenland Ice Sheet. *Geophysical Research Letters*, 44(22), 11463–11471. Available from: https://doi.org/10.1002/2017GL075958

Sumner, L.W., Amberg, A., Barrett, D., Beale, M.H., Beger, R., Daykin, C.A. et al. (2007) Proposed minimum reporting standards for chemical analysis: chemical analysis working group (CAWG) metabolomics standards initiative (MSI). *Metabolomics*, 3(3), 211–221. Available from: https://doi.org/10.1007/s11306-007-0082-2

Uetake, J., Naganuma, T., Hebsgaard, M.B., Kanda, H. & Kohshima, S. (2010) Communities of algae and cyanobacteria on glaciers in West Greenland. *Polar Science*, 4(1), 71–80. Available from: https://doi.org/10.1016/j.polar.2010.03.002

Viant, M.R., Ebbels, T.M.D., Beger, R.D., Ekman, D.R., Epps, D.J.T., Kamp, H. et al. (2019) Use cases, best practice and reporting standards for metabolomics in regulatory toxicology. *Nature Communications*, 10(1), 1–10. Available from: https://doi.org/10.1038/s41467-019-10900-y

Weisskopf, L., Schulz, S. & Garbeva, P. (2021) Microbial volatile organic compounds in intra-kingdom and inter-kingdom interactions. *Nature Reviews Microbiology*, 19(6), 391–404. Available from: https://doi.org/10.1038/s41579-020-00508-1

Wetz, M.S. & Wheeler, P.A. (2007) Release of dissolved organic matter by coastal diatoms. *Limnology and Oceanography*, 52(2), 798–807. Available from: https://doi.org/10.4319/LO.2007.52.2.0798

Wienhausen, G., Noriega-Ortega, B.E., Niggemann, J., Dittmar, T. & Simon, M. (2017) The exometabolome of two model strains of the Roseobacter group: a marketplace of microbial metabolites. *Frontiers in Microbiology*, 8(10), 1985. Available from: https://doi.org/10.3389/FMICB.2017.01985/FULL

Williamson, C.J., Anesio, A.M., Cook, J., Tedstone, A., Poniecka, E., Holland, A. et al. (2018) Ice algal bloom development on the surface of the Greenland Ice Sheet. *FEMS Microbiology Ecology*, 94(3), 1–10. Available from: https://doi.org/10.1093/femsec/fiy025

Williamson, C.J., Cook, J., Tedstone, A., Yallop, M., McCutcheon, J., Poniecka, E. et al. (2020) Algal photophysiology drives darkening and melt of the Greenland Ice Sheet. *Proceedings of the National Academy of Sciences of the United States of America*, 117(11), 5694–5705. Available from: https://doi.org/10.1073/pnas.1918412117

Wilson, S.L., Frazer, C., Cumming, B.F., Nuin, P.A.S. & Walker, V.K. (2012) Cross-tolerance between osmotic and freeze-thaw stress in microbial assemblages from temperate lakes. *FEMS Microbiology Ecology*, 82(2), 405–415. Available from: https://doi.org/10.1111/J.1574-6941.2012.01404.X

Wlodarska, M., Luo, C., Kolde, R., d'Hennezel, E., Annand, J.W., Heim, C.E. et al. (2017) Indoleacrylic acid produced by commensal Peptostreptococcus species suppresses inflammation. *Cell Host & Microbe*, 22(1), 25–37.e6. Available from: https://doi.org/10.1016/J.CHOM.2017.06.007

Yallop, M.L., Anesio, A.M., Perkins, R.G., Cook, J., Telling, J., Fagan, D. et al. (2012) Photophysiology and albedo-changing potential of the ice algal community on the surface of the Greenland Ice Sheet. *The ISME Journal*, 6(12), 2302–2313. Available from: https://doi.org/10.1038/ismej.2012.107

Zhang, F., Harir, M., Moritz, F., Zhang, J., Witting, M., Wu, Y. et al. (2014) Molecular and structural characterization of dissolved organic matter during and post cyanobacterial bloom in Taihu by combination of NMR spectroscopy and FTICR mass spectrometry. *Water Research*, 57, 280–294. Available from: https://doi.org/10.1016/J.WATRES.2014.02.051

Zhang, Z., Qu, C., Zhang, K., He, Y., Zhao, X., Yang, L. et al. (2020) Adaptation to extreme Antarctic environments revealed by the genome of a sea ice green alga. *Current Biology*, 30(17), 3330–3341.e7. Available from: https://doi.org/10.1016/j.cub.2020.06.029

SUPPORTING INFORMATION

Additional supporting information can be found online in the Supporting Information section at the end of this article.